

Surface EXAFS study of metastable magnetic thin films

D. Chandesris,^{a*} P. Le Fèvre,^a H. Magan^{a,b} and H. Jaffrès^c

^aLaboratoire pour l'Utilisation du Rayonnement Electromagnétique, Orsay, France, ^bService de Recherche sur les Surfaces et l'Irradiation de la Matière, CEA, Saclay, France, and ^cLaboratoire de Physique de la Matière Condensée, INSA, Toulouse, France. E-mail: chandesris@lure.u-psud.fr

Epitaxial thin films provide new opportunities to explore the relationship between structure and magnetism. The bidimensionnal character of magnetic films deposited on single-crystal substrates and the occurrence of singular crystallographic structures often confer on these systems electronic and magnetic properties that cannot be found in the bulk solids. Although shape anisotropy would favour an in-plane easy axis of magnetization for thin films, Ni layers deposited on Cu(001) present a perpendicular magnetic anisotropy in a very wide thickness range. It is shown that this can be explained by a distorted structure of Ni, originating from the strain induced by the epitaxy on the Cu substrate. In the field of low-dimensional magnetism, nanostructures with a reduced lateral dimension are now being widely investigated in view of their technological applications. Thin Fe layers on MgO(001) can be cut into strips by the 'atomic saw' method: a compression of the substrate induces a dislocation slipping which 'saws' both the substrate and the Fe film into regular and separated ribbons. The observed magnetic anisotropy, with the easy axis perpendicular to the strips, is explained by a structural relaxation occurring during the structuration process. In these two studies, a precise structural characterization and simple magnetoelastic models allow the magnetic behaviour of the systems to be described. The structure of the films can be described as an elastic deformation of the bulk structure.

Keywords: XAFS; thin films; magnetism.

1. Introduction

Thin films deposited on single-crystal substrates can be stabilized into novel crystallographic phases, thus creating a new class of materials with electronic and magnetic properties that cannot be found in the bulk solids. A clear explanation of the magnetic properties of thin films, as well as improvements of theoretical models, requires a precise characterization of the film crystallography. Surface extended X-ray absorption fine structure (surface EXAFS) is a technique particularly adapted to these studies. Two examples are presented here: Ni thin films deposited on Cu(001) and thin Fe layers deposited on MgO(001), patterned into ribbons by the atomic saw method.

2. Structure of Ni/Cu(001)

For magnetic transition-metal layers, the appearance of the easy axis of magnetization perpendicular to the film plane (perpendicular magnetic anisotropy, PMA) is a typical bidimensionnal effect. It has been observed in various systems (Heinrich *et al.*, 1987; Pescia *et al.*, 1987; Allenspach, 1994) but only up to a critical thickness, always of the order of a few monolayers (ML). The behaviour of the Ni/Cu(001) system is different: magnetic measurements have shown that, for Ni layers thinner than 7 ML, the easy axis of magnetization lies in

the film plane, but switches perpendicular to the film plane for larger thicknesses (Schulz & Baberschke, 1994; Huang *et al.*, 1994). All the models proposed to explain the thickness-dependent magnetic easy axis of the Ni/Cu(001) films have introduced magnetoelastic terms (Schulz & Baberschke, 1994; Bochi *et al.*, 1995, 1996; Jungblut *et al.*, 1994; Naik *et al.*, 1993), induced by a tetragonal structure of the Ni films. The origin of this distorted structure is the adaptation of the Ni lattice to the Cu one. Ni and Cu are both face-centred cubic (f.c.c.) metals, with lattice parameters of, respectively, 3.52 Å and 3.61 Å. Ni would adopt the Cu lattice parameter parallel to the interface, this lateral expansion of the cell inducing a longitudinal contraction. Such tetragonal structures have been observed in previous studies (Heckmann *et al.*, 1994; Idzerda & Prinz, 1996; Müller *et al.*, 1996; Platow *et al.*, 1999).

Ni thin films grown on Cu(001) have been characterized by polarization-dependent surface EXAFS. The strengths of EXAFS are well known: it is a selective method and allows one to measure lattice parameters in all the crystallographic directions with the same accuracy.

The experiment was carried out at the Ni K edge (8333 eV). Ni was deposited under ultra-high vacuum (UHV), at room temperature, on a clean Cu(001) single crystal. The EXAFS data were recorded *in situ* at 77 K, in the total-yield mode, using two incident angles of the X-rays: normal incidence and grazing incidence, with polarization of the X-ray respectively parallel and almost perpendicular to the surface plane.

The Fourier transforms of the spectra for 10 ML Ni/Cu(001) are shown in Fig. 1. The contribution of the first-neighbour (FN) shell is extracted by an inverse Fourier transform of the first peak. This contribution is fitted using the classical EXAFS formula to determine the FN distance. The contribution of each FN bond to the EXAFS signal is weighted by $\cos^2\alpha$, where α is the angle between the bond and the linear polarization of the X-rays. In grazing incidence, only the eight FN bonds out of the (001) planes (out-of-plane bonds) contribute to the signal, whereas in normal incidence, the four bonds contained in the (001) planes (in-plane bonds) and the eight out-of-plane bonds contribute with the same apparent weight. Fits of the two normal incidence and grazing incidence spectra allow us to determine both the in-plane and the out-of-plane FN bond lengths ($R_{\text{out-of-plane}}$ and $R_{\text{in-plane}}$). For all the studied Ni thicknesses (3 to 10 ML), we obtain $R_{\text{in-plane}} = 2.55 \pm 0.01$ Å, a value equal to the FN distance in the Cu substrate, and $R_{\text{out-of-plane}} = 2.50 \pm 0.01$ Å. From 3 to 10 ML, the Ni films are in a face-centred tetragonal (f.c.t.) structure, with lattice parameters parallel and perpendicular to the interface: $a_{\parallel} = 3.61 \pm 0.02$ Å and $a_{\perp} = 3.46 \pm 0.04$ Å.

This tetragonal structure is confirmed by observing the polarization dependence of the distant-neighbour shell contributions to the EXAFS signal. A simulation of the X-ray absorption spectra using the *FEFF6* code, which calculates the absorption cross section using a multiple-scattering formalism (Rehr *et al.*, 1991; Le Fèvre *et al.*, 1995) is shown in Fig. 1 with the experimental spectra. The best agreement was achieved with lattice parameters of $a_{\parallel} = 3.61$ Å and $a_{\perp} = 3.42$ Å, very close to those determined by the FN shell analysis. These values are also comparable with those measured in a recent low-energy electron diffraction study [$a_{\parallel} = 3.58$ Å and $a_{\perp} = 3.41$ Å (Platow *et al.*, 1999)].

3. Strain relaxation in Fe thin films patterned by the atomic saw method

Fe films of 50 Å thickness were epitaxially grown on an MgO(001) substrate in UHV: Fe grows in a body-centred cubic (b.c.c.)-like

structure on f.c.c. MgO(001) with the relative orientation MgO(001)[010]||Fe(001)[110]. As seen by RHEED (reflective high-energy electron diffraction (Durand *et al.*, 1995; Childress *et al.*, 1994), the 3.8% lattice mismatch should stretch the Fe lattice parallel to the interface. To avoid any oxidation of the Fe film, a 15 Å Pd layer was deposited on the Fe.

The so-called atomic saw method (Peyrade *et al.*, 1992; Goiran *et al.*, 1993) consists of applying a uniaxial compressive stress on a sample in order to induce plastic deformation, *i.e.* dislocation slipping through the whole system 'substrate and epitaxial film'. When dislocations cross the film, the layer is cut in separate strips. This method has been successfully used to cut Fe thin films, epitaxially grown on MgO(001), into strips and boxes (Jaffrès, Ressler, Peyrade *et al.*, 1998; Jaffrès, Ressler, Postava *et al.*, 1998). Fe ribbons aligned along the MgO [010] direction, corresponding to the [110] direction in the Fe film, were fabricated using a plastic strain equal to 8%. The analysis of atomic force microscopy images enabled the evaluation of the width L (100 ± 50 nm) and relative height h (1 ± 0.5 nm) of the ribbons. Magneto-optical measurements on the Fe 'sawed' film revealed a strong magnetic uniaxial anisotropy, characterized by an easy axis of magnetization perpendicular to the strips, which is unexpected from shape-energy considerations.

In the as-deposited films, the Fe b.c.c. structure is supposed to be laterally stretched by epitaxy on the MgO substrate. This lateral expansion induces a longitudinal compression of the cubic unit cell, leading to a body-centred tetragonal (b.c.t.) structure with lattice parameters a and c (Fig. 2*a*). Each Fe atom has four FN bonds located at R_3 in the same (100) plane, as well as eight FN bonds located at R_1 and two at R_2 out of this plane. In the patterned film, the atomic saw process could induce a relaxation of the Fe tetragonal cell perpendicular to the strips. This would lead to a monoclinic structure, as schematically presented in Fig. 2*b*), and described by three crystallographic parameters α' , β' and c' and FN distances R'_1 , R'_2 , R'_3 (Fig. 2*b*). This structure could explain the magnetic anisotropy.

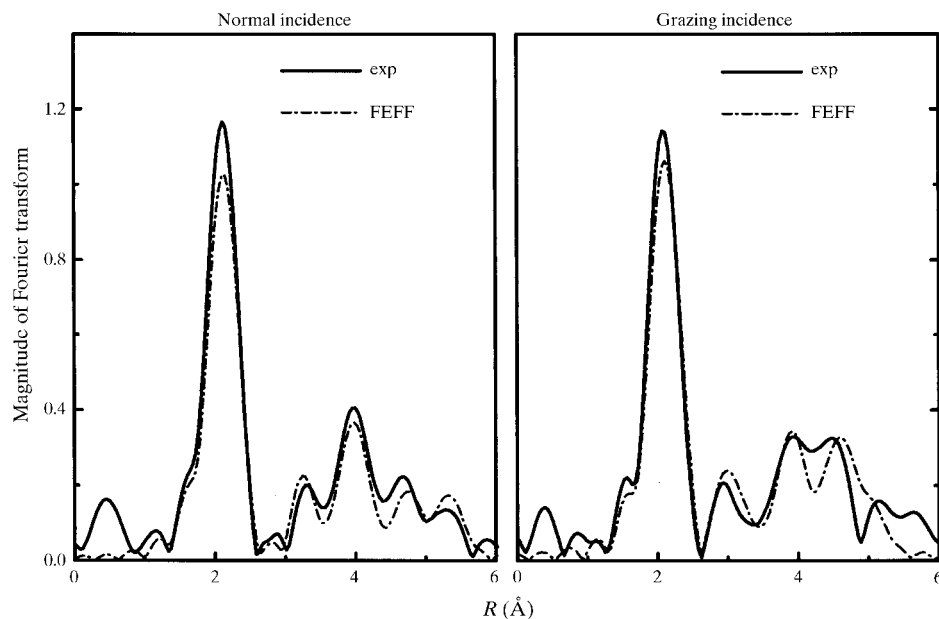


Figure 1 Fourier transform (between $k = 2.55$ and $k = 12.35 \text{ \AA}^{-1}$) of experimental EXAFS spectra recorded on a 10 ML Ni/Cu(001) film in normal incidence and in grazing incidence. Comparison with FEFF calculation using $a_{\parallel} = 3.61 \text{ \AA}$ and $a_{\perp} = 3.42 \text{ \AA}$.

We have used the polarization dependence of the EXAFS spectra to measure the different crystallographic parameters of these two distorted structures. The EXAFS spectra at the Fe K edge (7110 eV) were recorded *ex situ* at 77 K in the fluorescence-yield mode. For these distorted b.c.c. structures, whatever the X-ray angle of incidence, R_1 , R_2 and R_3 (or R'_1 , R'_2 , R'_3) being very similar distances, there are always two types of neighbours contributing to the FN EXAFS signal. Unlike for the study of Ni/Cu(001), there is no peculiar X-ray angle of incidence for which a unique bond length can be isolated. A fit of the FN contribution using classical EXAFS formulae would require too many parameters and would not be precise enough. We have therefore used the phase-derivative method (Martens *et al.*, 1977; Jiang *et al.*, 1991). When two different bond lengths (R_1 and R_2 for example) contribute to the FN EXAFS signal, as a result of the interference between the different shells, a kink occurs in the total phase when the value k of the wavevector of the photoelectron is approximately equal to $\pi/2(R_2 - R_1) = \pi/2\Delta R$. In practice, the kink position is located by taking the minimum of the derivative of the total phase with respect to k , and the precise determination of ΔR is performed by comparing the experimental phase derivative and a theoretical calculation performed with the FEFF code (Rehr *et al.*, 1991). We have tested this method on bulk Fe and have shown (Jaffrès *et al.*, 2000) that the accuracy on the ΔR determination is about 0.01 \AA .

This method is applied for the structure determination of the as-deposited film. Fig. 2*c*) shows the experimental phase derivative for the spectra recorded in normal incidence (NI) and in grazing incidence (GI). The different distances contributing to the signal are R_1 and R_3 in normal incidence, and R_1 and R_2 in grazing incidence. We have then $\Delta R_{\text{NI}} = R_3 - R_1$ and $\Delta R_{\text{GI}} = R_2 - R_1$. With $a > c$, one obtains $\Delta R_{\text{NI}} > \Delta R_{\text{GI}}$, and, therefore, a kink position at a smaller k value in normal incidence than in grazing incidence. This is clearly observed in the experiment and demonstrates the tetragonal structure of the as-deposited Fe film. We obtain a good agreement

between experiment and FEFF simulations for $a = 2.915 \pm 0.015 \text{ \AA}$ and $c = 2.82 \pm 0.01 \text{ \AA}$. As it was supposed above, in the as-deposited film, Fe is in a tetragonal structure, resulting from an epitaxially strained b.c.c. structure. The bonds parallel to the surface ($a = 2.915 \text{ \AA}$) are smaller than in MgO (2.98 \AA): this can be explained by a partial strain relaxation in the Fe film as indicated by the 'stand off' dislocations observed by high-resolution transmission electron microscopy (Snoeck *et al.*, 1998).

In the patterned Fe film, the Fe structure is expected to be monoclinic and described by three crystallographic parameters α' , β' and c' (Fig. 2*b*). For this sample, we have recorded three absorption spectra: a grazing-incidence spectrum, with the linear polarization of the X-rays perpendicular to the film plane, and two normal-incidence spectra, with the linear polarization of the X-rays parallel to the film plane, but either parallel (PA) or perpendicular (PE) to the strips. The FN contribution will be due to R'_1 , R'_2 and R'_3 in grazing inci-

dence, to R'_1 and R'_3 when the polarization is parallel to the strips, and to R''_1 and R''_3 when the polarization is perpendicular to the strips. We have used the phase-derivative method to analyse the data; the experimental spectra are shown in Fig. 2(c). The two spectra recorded with the polarization either parallel or perpendicular to the strips present minima located at different k values, denoting a non-square symmetry of the surface lattice. According to our notation, the bond length differences involved for each polarization direction are $\Delta R_{PE} = R'_3 - R'_1$, $\Delta R_{PA} = R'_3 - R'_1$ and $\Delta R_{GI} \simeq R'_2 - 1/2(R'_1 + R'_1)$.

As in the study of the as-deposited film, the crystallographic parameters (α' , β' , c') are obtained by comparing the experimental curves with *FEFF* simulations: the best agreement is reached for $\alpha' = 2.02 \pm 0.01$ Å, $\beta' = 2.07 \pm 0.01$ Å and $c' = 2.83 \pm 0.01$ Å.

These results show that the patterned film has a monoclinic structure. As it was supposed, the effect of the atomic saw process is mainly to relax the epitaxial strain perpendicular to the ribbons. Thus, the structure is also slightly relaxed perpendicular to the film plane ($c' > c$).

4. Structure of thin films as elastic deformation of bulk structure

In a previous study of Co films on Cu(001) (Heckmann *et al.*, 1994), the Co tetragonal structure was explained by an elastic deformation of a cubic cell, using the continuum elastic theory. In this approach, assuming that the thin films can be considered as an elastic continuum, the elastic theory is used to predict the contraction of the lattice parameter in the direction perpendicular to the interface,

knowing the strain imposed by the substrate. Since the surface of the film is free, there is no stress in the direction perpendicular to the interface. Therefore, a_{\perp} and a_{\parallel} in the tetragonal structure of Ni and a and c in the tetragonal structure of the as-deposited Fe film should be linked by the formulae (Hooke's law)

$$\frac{a_{\perp} - a_{\text{Ni}}}{a_{\text{Ni}}} = -2 \frac{C_{12}}{C_{11}} \frac{a_{\parallel} - a_{\text{Ni}}}{a_{\text{Ni}}}$$

and

$$\frac{c - a_{\text{Fe}}}{a_{\text{Fe}}} = -2 \frac{C_{12}}{C_{11}} \frac{a - a_{\text{Fe}}}{a_{\text{Fe}}},$$

where C_{ij} are the standard elastic coefficients of a cubic crystal and a_{Ni} and a_{Fe} are the lattice parameters of the bulk structures. For Ni films, a_{\parallel} was found to be imposed by the Cu substrate (3.61 Å) and, using $C_{12}/C_{11} = 0.578$ (Simmons & Wang, 1971), one obtains $a_{\perp} = 3.42$ Å. This leads to $R_{\text{out-of-plane}} = 2.49$ Å, a value very close to that determined by the EXAFS measurements. For the as-deposited Fe film, a is found to be 2.915 Å. Taking $C_{12}/C_{11} = 0.595$ (American Institute Handbook), one obtains $c = 2.82$ Å, a value also in agreement with the experimental measurement.

In the patterned Fe film, there are two stress-free directions: perpendicular to the surface and in the PE direction. Hooke's law then gives two equations,

$$\frac{\Delta\alpha}{\alpha} = \frac{\alpha' - \alpha_{\text{Fe}}}{\alpha_{\text{Fe}}} = -\frac{C_{11} + C_{12} - 2C_{12}^2/C_{11} - C_{44}}{C_{11} + C_{12} - 2C_{12}^2/C_{11} + C_{44}} \frac{\beta' - \beta_{\text{Fe}}}{\beta_{\text{Fe}}}$$

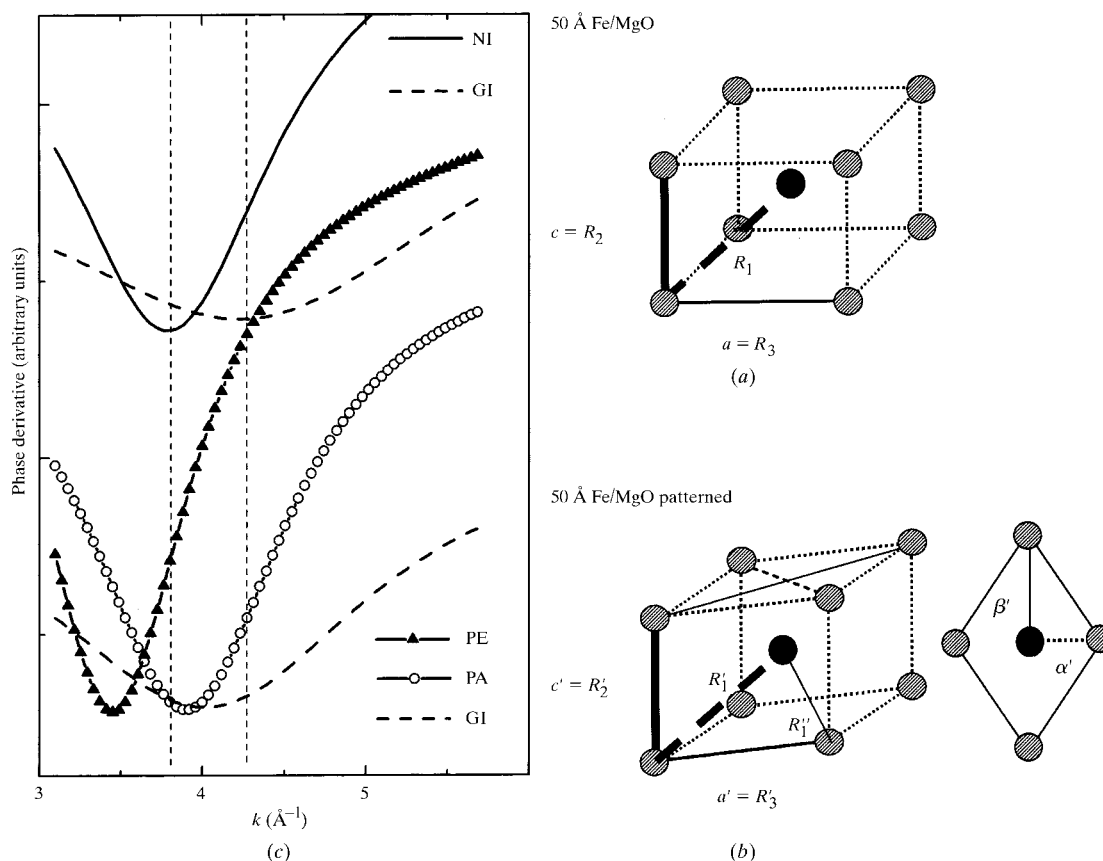


Figure 2 (a) Body-centred tetragonal (b.c.t.) structure expected in the case of the as-deposited film. (b) Trigonal structure expected for the patterned film. The b.c.t. cell is relaxed along the $[1\bar{1}0]$ direction. The projection in the (001) plane is shown; α' and β' are the values of the half diagonals. (c) Phase derivative of the first-neighbour EXAFS signal recorded in normal incidence (NI) and in grazing incidence (GI) on as-deposited Fe film (upper curves) and in perpendicular (PE), parallel (PA) and grazing incidence (GI) on the patterned Fe film (lower curves).

and

$$\frac{c' - c_{\text{Fe}}}{c_{\text{Fe}}} = -\frac{C_{12}}{C_{11}} \left(\frac{\Delta\alpha}{\alpha} + \frac{\Delta\beta}{\beta} \right),$$

where $\alpha_{\text{Fe}} = \beta_{\text{Fe}} = 2.03 \text{ \AA}$ and $c_{\text{Fe}} = 2.87 \text{ \AA}$ are the bulk Fe lattice parameters. Taking the numerical values (American Institute Handbook) of C_{ij} and the experimental $\beta' = 2.07 \text{ \AA}$, we found $\alpha' = 2.02 \text{ \AA}$ and $c' = 2.84 \text{ \AA}$. These values are again in perfect agreement with experimental values, showing that the main effect of the atomic saw process is to release the stress along the direction perpendicular to the strips.

5. Magnetoelastic model: Fe/MgO

The magnetoelastic energy in a cubic structure is

$$E_{\text{ME}} = B_1(\varepsilon_{11}M_x^2 + \varepsilon_{22}M_y^2) + 2B_2\varepsilon_{12}M_xM_y,$$

where B_1 and B_2 are the magnetoelastic coefficients. ε is the strain tensor and M_i are the magnetization coordinates on the standard Fe[100] basis. Also $\varepsilon_{12} = (1/2)(\Delta\alpha/\alpha - \Delta\beta/\beta)$. Then, the energy difference between the two in-plane magnetization directions (perpendicular or parallel to the strips) can be written

$$\Delta E_{\text{ME}} = B_2 \left(\frac{\Delta\alpha}{\alpha} - \frac{\Delta\beta}{\beta} \right) \simeq -1.9 \times 10^6 \text{ erg cm}^{-3},$$

with $B_2 = 7.62 \times 10^7 \text{ erg cm}^{-3}$ (Bruno, 1993). This negative value, obtained using the measured strains, shows that a magnetization vector perpendicular to the ribbons minimizes the magnetoelastic energy, as observed in the magneto-optical measurements. The anisotropy field H_a , given by $H_a = 2\Delta E_{\text{ME}}/M_s$, is roughly equal to 2250 Oe, a value very close to that determined experimentally (2400 Oe), which proves the validity of this simple magnetoelastic model.

A switching of the easy axis of magnetization has also been reported for Fe deposits on W(110) (Bansmann *et al.*, 1997; Lu *et al.*, 1998). The authors of those reports showed that an annealing of the Fe films resulted in the creation of elongated islands with an easy axis of magnetization that was different from that of the continuous as-deposited film. But, in these cases, the switching seemed to be caused by changes in the film morphology, and not structural effects as discussed here.

6. Conclusions

We have presented an EXAFS study on thin Ni and Fe films. In both cases, the epitaxy on a single-crystal substrate induces strains in the film. Despite a quite large strain parallel to the surface (2.6% in Ni films and 1.7% in Fe films), the Ni and Fe tetragonal or trigonal structures can be considered as elastic deformations of the bulk cubic cell, and are well described by the continuum elastic theory. These measurements are of key importance in order to understand the magnetic properties of these films. In both cases, one can show (Le Fèvre *et al.*, 1999; Jaffrès *et al.*, 2000) that simple magnetoelastic

models can account for the magnetic anisotropy observed in these samples.

References

- Allenspach, R. (1994). *J. Magn. Magn. Mater.* **129**, 160–185.
 Bansmann, J., Lu, L., Getzlaff, M. & Meiwes-Broer, K. H. (1997). *Z. Phys. D*, **40**, 570–573.
 Bochi, G., Ballentine, C. A., Inglefield, H. E., Thompson, C. V. & O'Handley, R. C. (1995). *Phys. Rev. B*, **52**, 7311–7321.
 Bochi, G., Ballentine, C. A., Inglefield, H. E., Thompson, C. V. & O'Handley, R. C. (1996). *Phys. Rev. B*, **53**, 1729–1732.
 Bruno, P. (1993). *Magnetismus von Festkörpern und Grenzflächen, Ferienkurse des Forschungszentrums*, Jülich, ch. 24.
 Childress, J. R., Kergoat, R., Durand, O., George, J. M., Galtier, P., Miltat, J. & Schuhl, A. (1994). *J. Magn. Magn. Mater.* **130**, 13–22.
 Durand, O., Childress, J. R., Galtier, P., Bisaro, R. & Schuhl, A. (1995). *J. Magn. Magn. Mater.* **145**, 111–117.
 Goiran, M., Guasch, C., Voillot, F., Carles, R., Peyrade, J. P., Bedel, E. & Munoz-Yague, A. (1993). *Europhys. Lett.* **23**, 647–652.
 Heckmann, O., Magnan, H., Le Fèvre, P., Chandresris, D. & Rehr, J. J. (1994). *Surf. Sci.* **312**, 62–72.
 Heinrich, B., Urquhart, K. B., Arrot, A. S., Cochran, J. F., Myrtle, K. & Purcell, S. T. (1987). *Phys. Rev. Lett.* **59**, 1756–1759.
 Huang, F., Kief, M. T., Mankey, G. J. & Willis, R. F. (1994). *Phys. Rev. B*, **49**, 3962–3971.
 Idzerda, Y. & Prinz, G. A. (1996). *Surf. Sci.* **284**, L394–L398.
 Jaffrès, H., Le Fèvre, P., Magnan, H., Midoir, A., Chandresris, D., Ressler, L., Schuhl, A., Nguyen Van Dau, F., Goiran, M., Peyrade, J. P. & Fert, A. R. (2000). *Phys. Rev. B*, **61**, 14628–14639.
 Jaffrès, H., Ressler, L., Peyrade, J. P., Fert, A. R., Gogol, P., Thiaville, A., Schuhl, A. & Nguyen Van Dau, F. (1998). *J. Appl. Phys.* **84**, 4375–4383.
 Jaffrès, H., Ressler, L., Postava, K., Schuhl, A., Nguyen Van Dau, F., Goiran, M., Redouler, J. P., Peyrade, J. P. & Fert, A. R. (1998). *J. Magn. Magn. Mater.* **184**, 19–27.
 Jiang, D. T., Crozier, E. D. & Heinrich, B. (1991). *Phys. Rev. B*, **44**, 6401–6409.
 Jungblut, R., Johnson, M. T., aan de Stegge, J., Reinders, A. & den Broeder, F. J. A. (1994). *J. Appl. Phys.* **75**, 6424–6426.
 Le Fèvre, P., Magnan, H. & Chandresris, D. (1999). *Eur. Phys. J. B*, **10**, 555–562.
 Le Fèvre, P., Magnan, H., Heckmann, O., Briosis, V. & Chandresris, D. (1995). *Phys. Rev. B*, **52**, 11462–11466.
 Lu, L., Bansmann, J. & Meiwes-Broer, K. H. (1998). *J. Phys. Cond. Mater.* **10**, 2873–2880.
 Martens, G., Rabe, P., Schwentner, N. & Werner, A. (1977). *Phys. Rev. Lett.* **39**, 1411–1414.
 Müller, S., Schulz, B., Kostka, G., Farle, M., Heinz, K. & Baberschke, K. (1996). *Surf. Sci.* **364**, 235–241.
 Naik, R., Kota, C., Payson, J. S. & Dunifer, G. L. (1993). *Phys. Rev. B*, **48**, 1008–1013.
 Pescia, D., Stampanoni, M., Bona, G. L., Vaterlaus, A., Willis, R. F. & Meier, F. (1987). *Phys. Rev. Lett.* **58**, 2126–2129.
 Peyrade, J. P., Voillot, F., Goiran, M., Atmany, H. & Rocher, A. (1992). *Appl. Phys. Lett.* **60**, 2481–2483.
 Platow, W., Bovensiepen, U., Pouloupolos, P., Farle, M., Baberschke, K., Hammer, L., Walter, S., Müller, S. & Heinz, K. (1999). *Phys. Rev. B*, **59**, 12641–12646.
 Rehr, J. J., Mustre de Leon, J., Zabinski, S. I. & Albers, R. C. (1991). *J. Am. Chem. Soc.* **113**, 5135–5140.
 Schulz, B. & Baberschke, K. (1994). *Phys. Rev. B*, **50**, 13467–13471.
 Simmons, G. & Wang, H. (1971). *Single-Crystal Elastic Constants and Calculated Aggregate Properties*, Cambridge Mass: MIT.
 Snoeck, E., Ressler, L., Jaffrès, H., Peyrade, J. P. & Schuhl, A. (1998). *J. Cryst. Growth*, **187**, 245–252.